Journal of Solid State Chemistry 186 (2012) 17–22

Contents lists available at SciVerse ScienceDirect

Journal of Solid State Chemistry

journal homepage: www.elsevier.com/locate/jssc

A green chemical approach to the synthesis of photoluminescent ZnO hollow spheres with enhanced photocatalytic properties

Greta Patrinoiu [a], Madalina Tudose [a], Jose Maria Calderón-Moreno [a], Ruxandra Birjega [b], Petru Budrugeac [c], Ramona Ene [a], Oana Carp [a,*]

[a] "Ilie Murgulescu" Institute of Physical Chemistry, Romanian Academy, Splaiul Independentei 202, 060021 Bucharest, Romania
[b] National Institute for Lasers, Plasma and Radiation Physics, P.O. BOX Mg—27, Magurele, Bucharest, Romania
[c] National Institute for Research and Development in Electrical Engineering, ICPE-CA, Advanced Research, Splaiul Unirii 313, 030138 Bucharest, Romania

ARTICLE INFO

Article history:
Received 22 August 2011
Received in revised form
7 November 2011
Accepted 14 November 2011
Available online 23 November 2011

Keywords:
Green synthesis
ZnO
Hollow spheres
Photoluminescence
Phenol degradation/mineralization

ABSTRACT

ZnO hollow spheres have been synthesized by a simple and environmentally friendly template assisted route. Starch-derived carbonaceous spheres were used as template, impregnated with $Zn(CH_3COO)_2 \cdot 2H_2O$ to obtain zinc-containing precursor spheres and thermally treatment at 600 °C, yielding hollow ZnO spherical shells. The precursor spheres and hollow shells were characterized by X-ray diffraction, FTIR spectroscopy, scanning electron microscopy, thermal analysis and room-temperature photoluminescence measurements. The hollow spherical shells with diameters of ~150 nm and wall thickness of ~20 nm, are polycrystalline, with a mean crystallite size of 22 nm, exhibiting interesting emission features, with a wide multi-peak band covering blue and green regions of the visible spectrum. The photocatalytic activities (under UV and visible light irradiations) of the ZnO spherical shells evaluated for the phenol degradation reaction in aqueous solutions are outstanding, a total phenol conversion being registered in the case of UV irradiation experiments.

1. Introduction

Zinc oxide, a non-toxic and bio-compatible semiconductor, with a wide band gap (3.37 eV) and high exciton binding energy (60 meV) may be obtained with various morphologies [1], esthetically beautiful and also attractive due to their shape and size induced properties and applications [2–5]. Currently, one of the most important research directions is the development of new synthetic approaches of various ZnO nanomaterials morphologies [6], in which the synthesis can be easily controlled, in a green context materials' particularities such as size, shape, etc. and preliminary properties to other material characteristics (like optical, (photo)catalytical, etc.). The use of diverse polysaccharides (non-toxic compounds, renewable and widely available in great amounts) in oxides synthesis as stabilizers and templates may represent a resourceful green approach of advanced materials *design*/synthesis [7]. Among polysaccharides, starch (the second biopolymer in abundance after cellulose) occupies a special position because its twofold constituents: the linear amylase (α-1,4 glycosidic bonds) responsible for starch gelling and the branched amylopectine (α-1,4 and α-1,6 glycosidic bonds) accountable for its solubility. Analyzing the literature data referring strictly to the synthesis of zinc oxide in the presence of starch we can mention successful procedures like precipitation [8] and sonochemical [9] in obtaining solid spheres and flower-like ZnO structures.

One of the most interesting ZnO structures are hollow spheres, due to their diverse applications such as drugs delivery, catalysis, chemical storage, microcapsule reactors, photo-electric materials, etc. [10–12]. In general, synthetic methods toward hollow structures can be classified into two types: template-free methods based on oriented attachment [13], Kirkendall effect [14], Ostwald ripening [15] and soft [16] /hard [17,18] template-directed synthetic routes.

Lately, carbonaceous spheres have been obtained through hydrothermal treatments of different precursors, including small chain hydrocarbons [19,20], simple organic acids [21] or corn oil [22]. The hydrothermal carbonization of carbohydrates, mainly glucose [11,23], have demonstrated their usefulness for obtaining sacrificial template carbonaceous spheres; thanks to three key unique features: (i) hydrophilicity inherited from the starting carbohydrate, (ii) tailor-made size and shape, achieved by a convenient variation of synthesis parameters and (iii) eco-friendly nature [24,25]. Starch is a cheaper and more available saccharide than glucose, but its low water solubility limited the use as precursor for spheroidal, solid, carbon-rich templates. In spite of this drawback, several high and moderate-temperatures solvo/hydrothermal procedures were

* Corresponding author. Fax: +40 213121147.
E-mail address: ocarp@icf.ro (O. Carp).

0022-4596/$ - see front matter © 2011 Elsevier Inc. All rights reserved.
doi:10.1016/j.jssc.2011.11.024

developed. A hydrothermal synthesis performed at a temperature of 600 °C determines the synthesis of monodisperse carbon microsphere with sizes of about 2 μm [26]. An alcohol (ethanol, *n*-propanol, *n*-butanol, 1-pentanol and 1-octanol) reaction medium functions as well as a structure-directing agent that controls the self-assembly of carbon colloids to spheroidal particles with shapes depending on alcohol nature (rugby-ball-like, lemon-like, oblate and fusiform spheroidal), at a reaction temperature of 550 °C [25]. Hydrothermal synthesis accomplished at moderate temperatures (170–240 °C) lead to spherical particles more or less interconnected [27]; the literature mentions also several attempts in elucidation of the reaction mechanisms [27,28].

On the other hand, the selection of the coating raw material and procedure is a critical step in obtaining hollow spheres. Metal acetates characterized by versatile linking abilities (coordination/chelation, hydrogen bonding) as well as high water solubility, low conversion temperatures and not least, low prices, represent without doubt an appropriate choice [29]. Thus far, zinc acetate was used with success in precipitation [30] and sonochemical (dimethylformamide [31] and water [11,32] reaction media) deposition approaches.

Herein, we report a novel, simple environmental friendly routine for large scale synthesis of ZnO hollow structures, characterized by interesting photoluminescent and photo- and catalytical properties. The synthetic route involves the formation of monodisperse, starch- derived carbonaceous sacrificial template and a facile, reproducible impregnation procedure as deposition technique. The synthesis is totally green being performed in aqueous solution, without using any stabilizer, alkali, surfactant or other toxic reagents and, during the calcination procedure mainly CO_2 (besides water), an environmentally circular gas is evolved. The obtained ZnO hollow spheres, characterized by visible emission features, were tested as photocatalyst in phenol degradation/mineralization from aqueous solution at room temperature.

2. Experimental

2.1. Hollow spheres synthesis

The compounds zinc acetate dehydrate $Zn(CH_3COO)_2 \cdot 2H_2O$ (Reactivul) and starch (Carl Roth Gmbh) were used as received.

In a typical starch-derived carbonaceous spheres synthesis, a starch aqueous solution with a slightly opalescent aspect is formed by starch dissolution in hot water. Our experiments covered a starch concentration within 0.1–0.4 M range. 20 ml of the above aqueous solution is sealed in a 25 mL teflon-lined autoclave and heated for 12–24 h in the temperature interval 160–180 °C. The final black products, collected by centrifugation, were washed with double distilled water and ethanol several times and dried at 60 °C/5 h.

For impregnation, the as-prepared starch-carbonaceous spheres (0.2 g), uniformly dispersed in 57 ml of distilled water by ultrasonication (15 min), were mixed with a solution of 50 ml of distilled water containing 1.8 g $Zn(CH_3COO)_2 \cdot 2H_2O$ (weight ratio starch/carbonaceous spheres equal with 1/9). The afore mentioned solution was magnetically stirred 4 h, and subsequently aged 48 h at ambient temperature yielding zinc acetate impregnated spheres (ZAI). Finally, the powders were thermally treated at 600 °C/1 h (heating rate of 3 °C/min).

2.2. Characterization

FTIR spectra (KBr pellets) were recorded with a FTIR Brucker Tensor V-37 spectrophotometer.

Thermal measurements were performed on a Netzch thermo balance STA 409 PC/PG type, in static air, with a heating rate of 10 °C/min with sample mass of ~10 mg.

X-ray diffraction measurements were carried out at room temperature on a PANalytical X'Pert PRO MPD X-ray diffractometer. Incident X-ray radiation was line focused Cu X-ray tube providing a $K\alpha$ wavelength of 1.5418 Å. A curved graphite monochromator and a 1° progressive divergence slit were placed in the diffracted beam. A continuous scan mode with a step size of 0.02° 2θ *counting* 20 s on each step was used.

Photoluminescence (PL) measurements were performed on a JASCO FP 6500 spectrophotometer, using 340-nm excitation line of xenon light.

Scanning electron microscopy (SEM) measurements were carried out in an environmental SEM Zeiss EVO LS10 and in a field emission SEM Hitachi H-4100FE (Tokyo, Japan).

2.2.1. Photocatalytical activity

The phenol degradation was investigated using stationary quartz reactors and UV (60 W, filter at $\lambda = 365$ nm) and visible (60 W, $\lambda > 380$ nm) lamps. The photocatalytic activity were evaluated from conversion of phenol in aqueous solution at 0.002 M concentration. Prior to irradiations, the suspensions were magnetically stirred in dark for 10 min, in order to reach adsorption-desorption equilibrium. The reactors were maintained at room temperature and under continuous magnetic stirring for all experiments. The distance between the light source and the reaction tube was 8 cm. The reaction products were filtered through Millipore membrane filters and analyzed on a DANI GC 1000 gas chromatograph connected to a FID detector.

3. Results and discussions

3.1. Precursors synthesis and characterization

The starch derived carbonaceous spheres were prepared under hydrothermal conditions at temperatures (160–180 °C) higher than the normal glycosidation temperature in order to allow the progress of successive aromatization and carbonization processes [33]. The size (diameters) of the carbonaceous spheres could be easily modulated through the variation of the hydrothermal parameters (mainly reaction time but also reaction temperature and starch concentration). In our experimental conditions diameters ranging between 250 and 800 nm were obtained. The lowest values were obtained after 12 h of hydrothermal reaction (Fig. 1a), while higher reaction time (24 h) and a starch concentration of 0.4 M lead to the formation of bigger and interconnected spheres (Fig. 1b).

Due to an incomplete carbonization process [34], the starch-derived carbonaceous spheres have abundant surface functional groups (hydroxyl, carboxyl), with enhanced bonding abilities toward other functional groups and molecules. The presence of hydroxyls groups is evidenced on the uncoated spheres (Fig. 2) by the strong wide peak at 3420 cm^{-1} attributed to the O–H (hydroxyl, carboxyl) bending vibrations, whereas the bands in the range 1050–1450 cm^{-1} region corresponds to C–O stretching (ester, ether) and O–H bending vibrations [23]. The other two important bands from 1700 and 1620 cm^{-1} are attributed to C=O (carbonyl, quinine, ester and carboxyl) and C=C vibrations [35]. Acetate characteristic bands, namely $\nu_{asym}(COO^-)$ and $\nu_{sym}(COO^-)$, positioned at 1558 and 1447 cm^{-1} in $Zn(CH_3COO)_2 \cdot 2H_2O$ raw material cannot be clearly identified in zinc acetate impregnated spheres (Fig. 2b) because their overlapping with spheres absorption peaks. However, the linkage between the zinc acetate and template, by hydrogen/coordination bonds, is supported by the

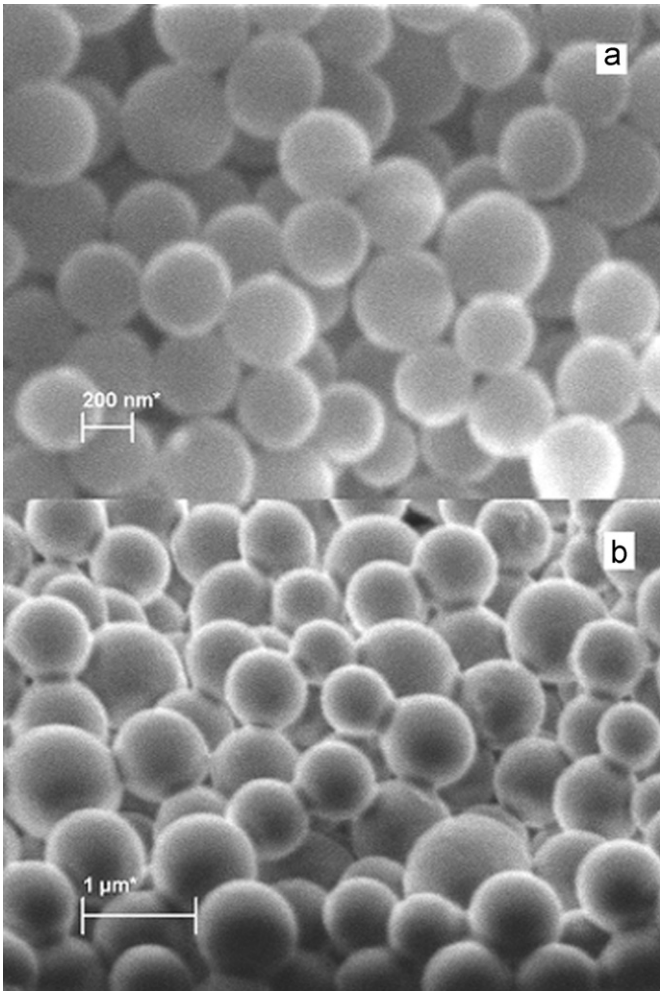

Fig. 1. Starch derived spheres: (a) 0.3 M starch, $T=180$ °C, $t=12$ h; (b) 0.4 M starch, $T=180$ °C, $t=24$ h.

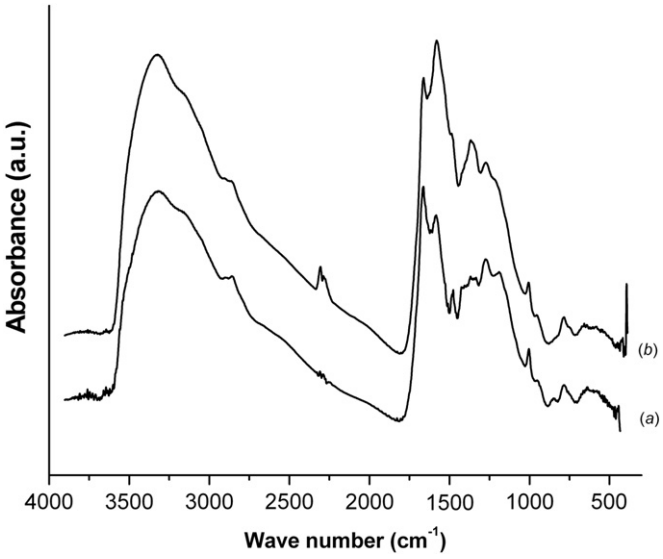

Fig. 2. FTIR spectra of carbonaceous spheres: (a) uncoated and (b) impregnated with $Zn(CH_3COO)_2 \cdot 2H_2O$ (starch 0.3 M, $T=180$ °C, $t=24$ h).

three clues: (i) an increased intensity of the ν(C═C) band with maximum at 1620 cm^{-1} due to the overlapping with acetate $\nu_{asym}(COO^-)$ vibration, (ii) weaken absorption peaks of O–H

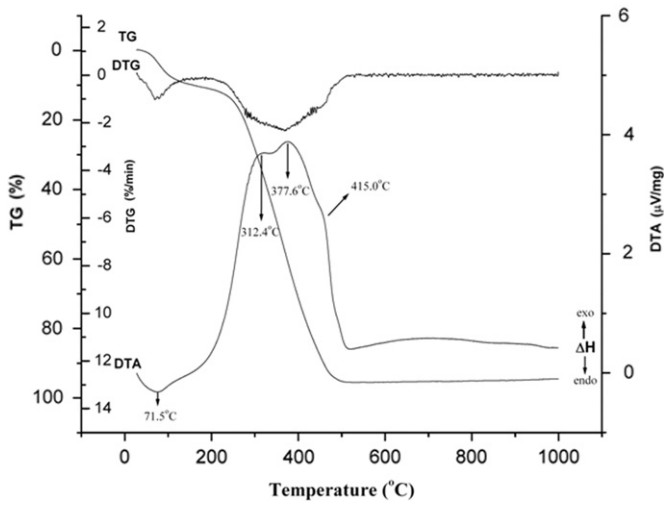

Fig. 3. Thermoanalytical curves (TG, DTG and DTA) of the core/shell precursors (starch 0.3 M, $T=180$ °C, $t=24$ h).

bending vibrations in the range 1200–1300 cm^{-1} determined by the hydroxyls bonding to Zn^{2+} and (iii) the appearance of a new band at 401 cm^{-1} assigned to Zn–O vibration.

Thermal analysis investigations of the coated spheres were performed in order to determine their thermoreactivity (especially the final decomposition temperature) and to establish the amount of zinc acetate bonded to the carbonaceous compound.

The decomposition takes place in the temperature range 42.5–502.0 °C. The registered total weight loss is 92.26% (Fig. 3), meaning that only part of the dissolved zinc acetate is bonded to the carbonaceous spheres: a carbonaceous spheres/$Zn(CH_3COO)_2 \cdot 2H_2O$ weight ratio of approximately 4 characterized the as prepared core/shell spheres. Two weight loss processes are clearly observed in the thermoanalytical curves (TG, DTG and DTA): the first process, associated with an endothermic effect (weight loss=10.43%, 42.5–173.5 °C), is ascribed to dehydration, while the second one (173.5–502.0 °C) comprising three exothermic effects, represents acetate decomposition and carbonaceous spheres degradation. No phase transition is registered on the DTA curve, indicating that ZnO crystallization occurs simultaneously with decomposition progress. A mass gain of 2.26% is registered after the end of degradation stages (502–700 °C), credited to the adsorption of the environmental gaseous products on the reactive oxide surface.

The morphology of the ZAI carbonaceous spheres studied by SEM. Fig. 4a–c shows the ZAI spheres obtained using a starch solution of 0.3 M a hydrothermal temperature and time equal with 180 °C and 24 h.

3.2. ZnO hollow spheres characterization

A typical XRD pattern of the product obtained after the calcination of the ZAI spheres for one hour at 600 °C is presented in Fig. 5, compared with the XRD profile of ZnO powder (Merck) used as reference. The mean crystallite size was calculated from the XRD patterns, averaging all reflections using the Scherrer formula from the instrumental corrected full width at half maximum. A 22 nm was obtained for ZnO hollow spheres to be compared with 74 nm determined for the reference ZnO powder from Merck.

The SEM analysis of the thermally treated spheres determined a distinct morphology of spherical shells (Fig. 6). The thermally treated sample shows a spherical morphology (Fig. 6a, c and e). We determined that they were hollow structure after grinding in a mortar shortly to break the spherical ZnO bodies (Fig. 6b, d

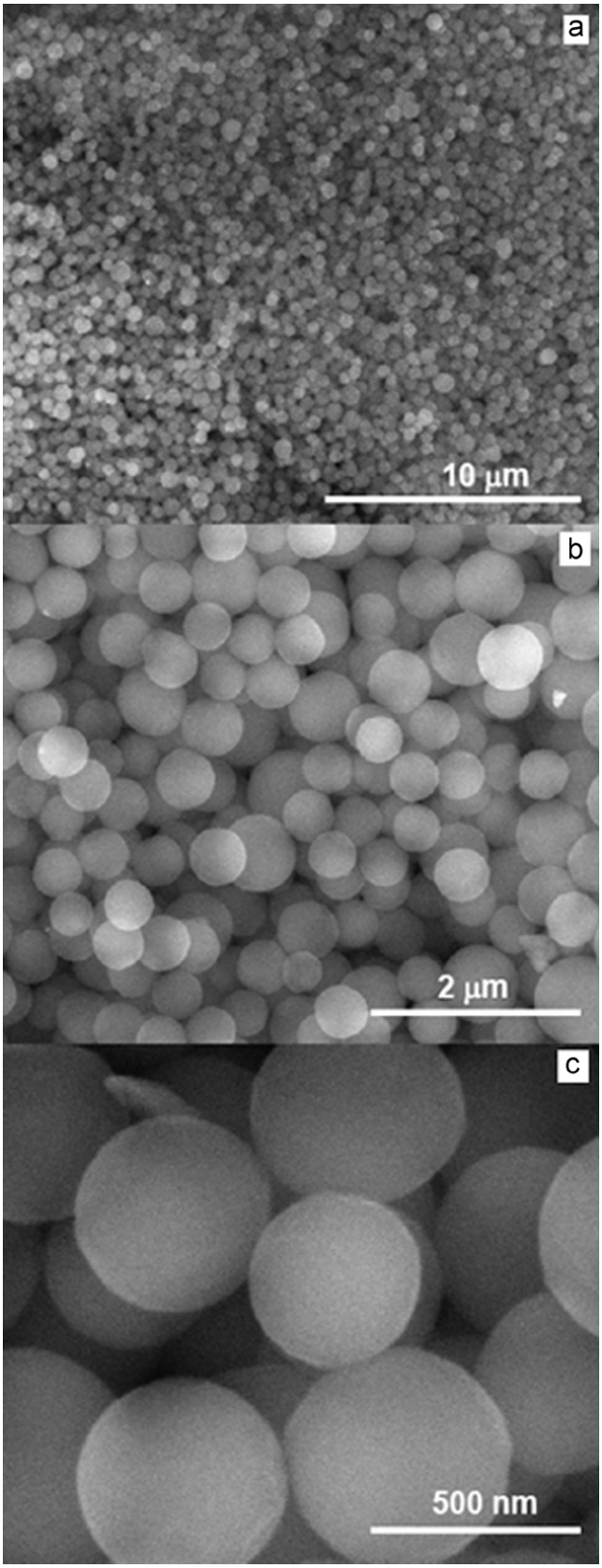

Fig. 4. SEM images of ZAI carbonaceous spheres (starch 0.3 M, $T=180$ °C, $t=24$ h).

and f). ZnO spherical shells have diameters between 150 and 200 nm, and the thickness of the ZnO shells is ~20 nm, close to the ZnO crystallites mean size obtained from X-ray diffraction

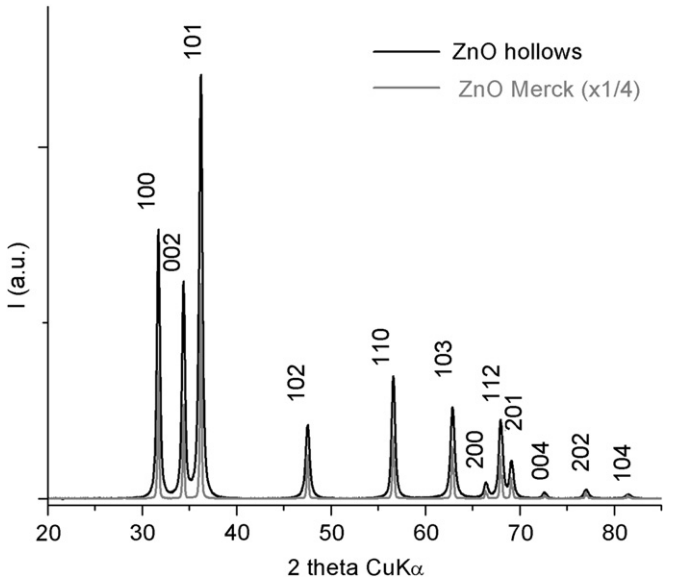

Fig. 5. XRD pattern of ZnO hollow microspheres (starch 0.3 M, $T=180$ °C, $t=24$ h) compared with the XRD pattern of a powder ZnO (Merck), recorded under the same conditions and presented 1/4 reduced.

measurements. It is worth to mention that sizes smaller than 200 nm of the hollow structures recommend them for biomedical applications; generally such dimensions are not obtained *via* template mediated approaches (using silica or polymer particles as templates), due to the difficulties arisen in the synthesis of small sized templates [12,36].

Room temperature photoluminescence spectrum of the ZnO hollow spheres presented in Fig. 7 shows only a wide band emission covering the blue–green regions, while the exciton-related near-band edge emission is absent. The mechanism behind visible photoluminescence is still unclear, but we attribute the increased visible emissions to the high density of surface defects (oxygen vacancies, zinc vacancies, oxygen interstitials and zinc interstitials) of the peculiar morphology described by a high surface-to-volume ratio [37]. This kind of multi-peaks PL spectrum in the visible region has been rarely reported, being identified for cuboid-shaped ZnO hierarchical structures [38], micro and nano-sized pencil-like ZnO [39] and ZnO hollow spheres assembled from 1D nanorods [40]. It is worth to mention, that a high density of surface defects is a prerequisite for photocatalytic applications of these materials, surface defects being responsible for the increase in lifetime of the charge carriers and hence an increase in the photocatalytic activity [41].

3.3. Photocatalytical activity

To validate ZnO hollow spheres potential for environmental applications such as removal of organic compounds from wastewater, their photocatalytical activities were investigated towards phenol oxidation, a toxic compound commonly used as solvent or reagent in many industrial processes [42,43].

The energy levels of the conduction and valence bands and the electron affinity of zinc oxide are similar to those of TiO_2, making ZnO an expected candidate as a semiconductor material for photocatalysis. It is also anticipated that nanostructured ZnO may be developed into a versatile alternative to TiO_2 (sometimes much more efficient), particularly for photocatalytic degradations of some azo dyes [44,45] and pulp wastewaters [46] under UV irradiation. The literature mentions already partial degradation/mineralization of phenol during photocatalytical processes, under UV and visible (solar or artificial irradiation) [47–52] sometimes

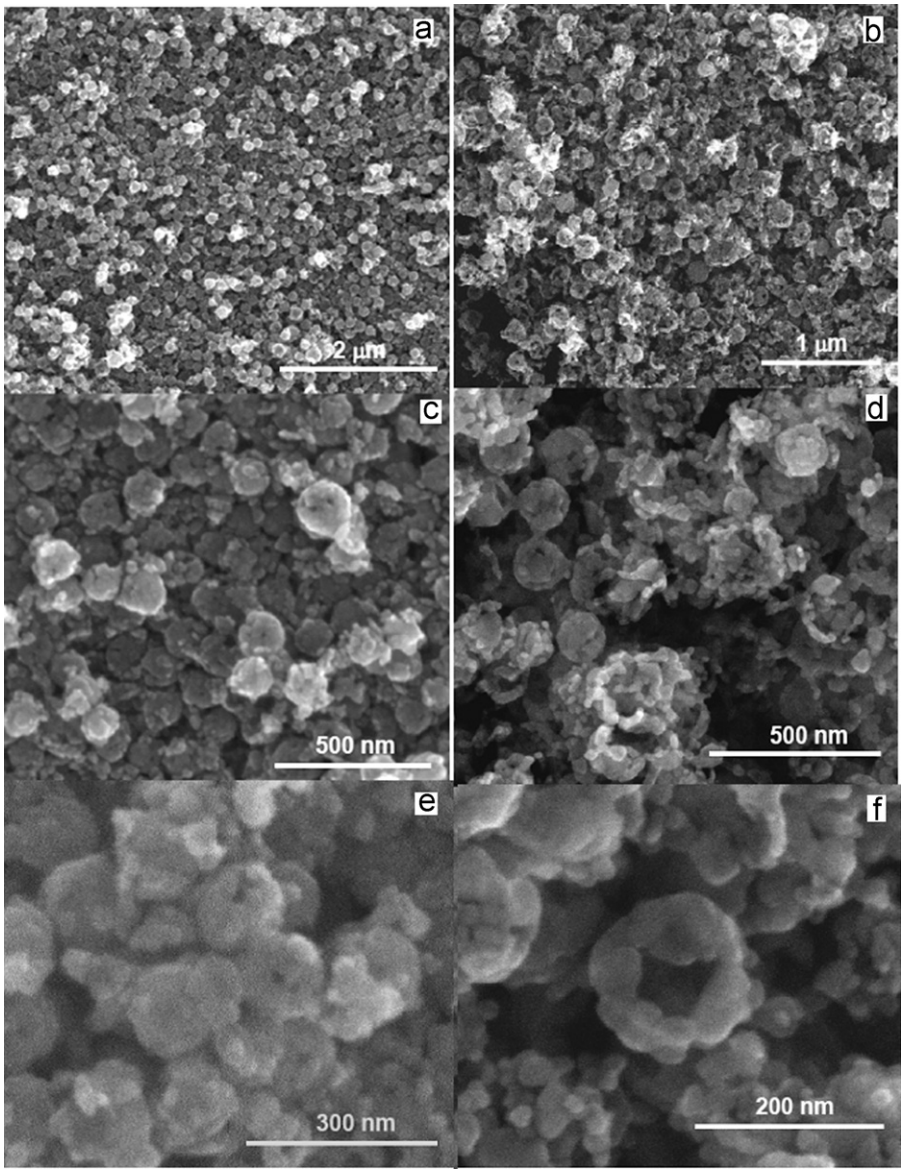

Fig. 6. SEM images of ZnO hollow spheres: (a, c, e) as obtained; after grinding (b, d, f).

in the presence of different oxidants such as manganese oxides (α-MnO_2, β-MnO_2 and δ-MnO_2) [53] or persulfate based compounds [54].

To our knowledge, the present study is the first that reports the photocatalytical activity of ZnO hollow spheres, evaluated in a test experiment as phenol photodegradation. Fig. 8 presents comparative the phenol photocatalytic conversions obtained during different irradiations (UV-365 nm and visible radiation) for the ZnO hollow spheres and a control sample of commercial ZnO (Merck) with a wide size range of 50–500 nm (Fig. 1 of Supplementary data). The photocatalytical activity of the ZnO is superior to the control sample. Two features define the photocatalytic performance of the ZnO hollow spheres: the high obtained conversion degrees, over 80% under visible irradiation and a total one in UV (365 nm) conditions, and the large percentage of phenol mineralization reactions, 85% in UV and 100% in visible. The organic products evidenced in UV conditions were hydroquinone and catechol (15%).

The photocatalytic reaction initiated by the photoexcitation of the semiconductor (ZnO) leads to the formation of electron–hole, while part of the electron–hole pairs recombines, some holes combine with water to form •OH radicals and some electrons convert oxygen to super oxide radical ($\bullet O_2^-$). Both •OH radicals and super oxide radicals are strong oxidizing species, which leads to the partial or complete mineralization of several organic chemicals [55]. An increase in the surface defects greatly reduces the direct recombination of photogenerated electron–hole pair [56], improving the photocatalytic activity. Thus, the enhanced photocatalytic activity of hollow ZnO is attributed to the increase in the surface defects as observed from enhanced emission peaks in the visible region of the photoluminescence spectra (Fig. 7).

4. Conclusions

In summary, here we demonstrate an environmentally friendly, facile, versatile and low cost template-directed synthesis of uniform ZnO hollow spheres. Starch, a very abundant, low-cost, nontoxic and renewable biopolymer, was used for template obtaining, and as zinc source $Zn(CH_3COO)_2 \cdot 2H_2O$. The developed procedure represents a rational synthetic green-alternative for the preparation of ZnO hollow spheres, being generally extendable to the

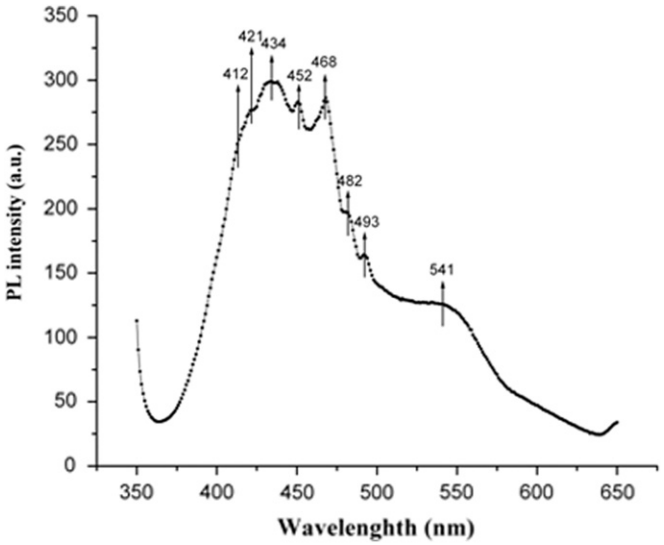

Fig. 7. Room-temperature photoluminescence spectra of ZnO hollow spheres (starch 0.3 M, T=180 °C, t=24 h).

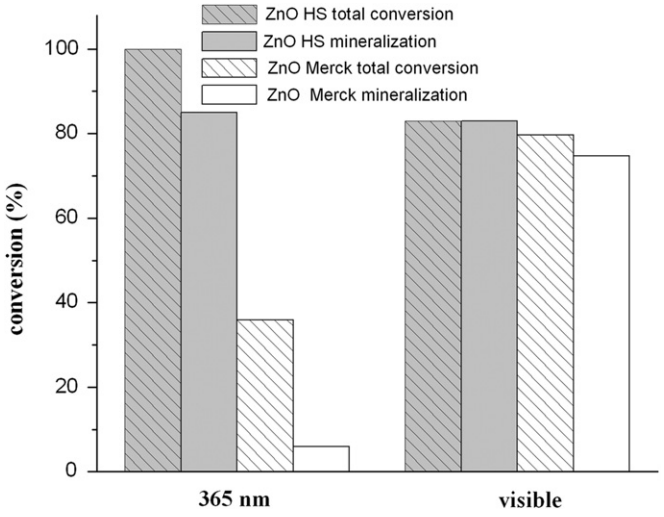

Fig. 8. Effects of ZnO nature and irradiation conditions on degradation of phenol.

synthesis of other inorganic hollow spheres, investigations that are in progress. The prepared ZnO hollow spheres present notable visible photoluminescence properties and remarkable photocatalytical activity in degradation/mineralization of phenol from wastewaters. The results show that organic compounds can be effectively mineralized to CO_2 and H_2O by the prepared ZnO hollow sphere photocatalysts under UV irradiation.

Acknowledgments

This work was supported by a Grant of the Romanian National Authority for Scientific Research, CNCS-UEFISCDI, Project number PN-II-ID-PCE-2011-3-0473. The paper was done within the research program "Coordinative and supramolecular chemistry" of the "Ilie Murgulescu" Institute of Physical Chemistry of the Romanian Academy.

Appendix A. Supplementary material

Supplementary data associated with this article can be found in the online version at doi:10.1016/j.jssc.2011.11.024.

References

[1] Z.L. Wang, Mater. Today 26 (2004) 26–33.
[2] M. Mo, J.C. Yu, L.Z. Zhang, S.K. Li, Adv. Mater. 17 (2005) 756–760.
[3] D.P. Norton, Y.W. Heo, M.P. Ivill, K. Ip, S.J. Pearton, M.F. Chisholm, T. Steiner, Mater. Today 34 (2004) 34–40.
[4] L. Schmidt-Mende, J.L. MacManus-Driscoll, Mater. Today 10 (2007) 40–48.
[5] Z.L. Wang, ACS Nano 2 (2008) 1987–1992.
[6] S.S. Warule, N.S. Chaudhari, B.B. Kale, M.A. More, Cryst. Eng. Commun. 11 (2009) 2776–2783.
[7] D. Visinescu, G. Patrinoiu, A. Tirsoaga, O. Carp, in: Eric Lichtfouse, Jan Schwarzbauer, Robert Didier (Eds.), Environmental Chemistry for a Sustainable World, vol. 2, 1st edition, Springer, ISBN: 978 94 007 2438 9.
[8] A. Taubert, G. Wegner, J. Mater. Chem. 12 (2002) 805–807.
[9] P. Mishra, R.S. Yadav, A.C. Pandey, Ultrason. Sonochem. 17 (2010) 560–565.
[10] K. An, T. Hyeon, Nano Today 4 (2009) 359–373.
[11] J. Zhang, S. Wang, Y. Wang, M. Xu, H. Xia, S. Zhang, W. Huang, X. Guo, S. Wu, Sens. Actuators B: Chem. 139 (2009) 411–417.
[12] X.W. Lou, L.A. Archer, Z. Yang, Adv. Mater. 20 (2008) 3987–4019.
[13] B. Liu, H.C. Zeng, J. Am. Chem. Soc. 126 (2004) 8124–8125.
[14] J.H. Yang, L.M. Qi, C.H. Lu, J.M. Ma, H.M. Cheng, Angew. Chem. Int. Ed. 44 (2005) 598–603.
[15] X.W. Lou, Y. Wang, C.L. Yuan, J.Y. Lee, L.A. Archer, Adv. Mater. 18 (2006) 2325–2329.
[16] D. Walsh, B. Lebeau, S. Mann, Adv. Mater. 11 (1999) 324–328.
[17] K.H. Rhodes, S.A. Davies, F. Caruso, B. Zhang, S. Mann, Chem. Mater. 12 (2000) 2832–2835.
[18] R.A. Caruso, Top. Curr. Chem. 226 (2003) 91–118.
[19] V.G. Pol, J.M. Calderón-Moreno, Carbon 42 (2004) 111–116.
[20] V.G. Pol, S.V. Pol, J.M. Calderón-Moreno, A. Gedanken, Carbon 44 (2006) 3285–3292.
[21] V.G. Pol, J.M. Calderón-Moreno, P.J. Chupas, R.E. Winans, P. Thiyagarajan, Carbon 47 (2009) 1050–1055.
[22] B. Basavalingu, J.M. Calderón-Moreno, K. Byrappa, Y.G. Gogotsi, M. Yoshimura, Carbon 39 (2001) 1763–1767.
[23] X. Sun, Y. Li, Angew. Chem. Int. Ed. 43 (2004) 3827–3831.
[24] X.L. Li, T.J. Lou, X.M. Sun, Y.D. Li, Inorg. Chem. 43 (2004) 5442–5449.
[25] M. Zheng, Y. Liu, K. Jiang, Y. Xiao, D. Yuan, Carbon 48 (2010) 1224–1233.
[26] M. Zheng, Y. Liu, Y. Xiao, Y. Zhu, Q. Guan, D. Yuan, J. Zhang, J. Phys. Chem. C 113 (2009) 8455–8459.
[27] M.M. Titirici, M. Antonietti, N. Bacile, Green Chem. 10 (2008) 1204–1212.
[28] M. Sevilla, A.B. Fuertes, Chem. Eur. J. 15 (2009) 4195–4203.
[29] T.J. Gardner, G.J. Messing, Thermochim. Acta 78 (1984) 17–27.
[30] H. Zhou, T. Fan, D. Zhang, Micropor. Mesopor. Mater. 100 (2007) 322–327.
[31] J. Zhang, S. Wang, Y. Wang, M. Xu, H. Xia, S. Zhang, W. Huang, X. Guo, S. Wu, Sens. Actuators B: Chem. 139 (2009) 411–417.
[32] X. Jia, H. Fan, F. Zhang, L. Qin, Ultrason. Sonochem. 17 (2010) 284.
[33] G.C.A. Luijkx, F. van Rantwijk, H. van Bekkum, M.J. Antal, Carbohydr. Res. 272 (1995) 191–202.
[34] Y.J. Zhan, S.H. Yu, J. Phys. Chem. C 112 (2008) 4024–4028.
[35] Q. Wang, H. Li, L.Q. Chen, X.J. Huang, Carbon 39 (2001) 2211–2214.
[36] K. An, T. Hyeon, Nano Today 4 (2009) 351–373.
[37] K. Vanheusden, C.H. Seager, W.L. Warren, D.R. Tallant, J.A. Voigt, Appl. Phys. Lett. 68 (1996) 403–406.
[38] D. Wang, Y. Zhao, C. Song, Solid State Sci. 12 (2010) 776–782.
[39] V.G. Pol, J.M. Calderón-Moreno, P. Thiyagarajan, Langmuir 24 (2008) 13640–13645.
[40] S.Y. Gao, H.J. Zhang, X.M. Wang, R.P. Deng, D.H. Sun, G.L. Zheng, J. Phys. Chem. B 110 (2006) 15847–15852.
[41] D.S. Bohle, C.J. Spina, J. Am. Chem. Soc. 131 (2009) 4397–4404.
[42] M.L. Davi, F. Gnudi, Water Res. 33 (1999) 3213–3219.
[43] K. Verschueren, Handbook of Environmental Data on Organic Chemicals, Van Nostrand Reinhold Co., New York, 1977.
[44] A. Akyol, H.C. Yatmaz, M. Bayramoglu, Appl. Catal. B: Environ. 54 (2004) 19–24.
[45] N. Daneshvar, D. Salari, A.R. Khataee, J. Photochem. Photobiol. A: Chem. 162 (2004) 317–332.
[46] M.C. Yeber, J. Rodriguez, J. Freer, J. Baeza, N. Duran, H.D. Mansilla, Chemosphere 39 (1999) 1679–1688.
[47] K. Hayat, M.A. Gondal, M.M. Khaled, S. Ahmed, A.M. Shemsi, Appl. Catal. A: Gen. 393 (2011) 122–129.
[48] S.K. Pardeshi, A.B. Patil, Sol. Energy 82 (2008) 700–705.
[49] K.M. Parida, S. Parija, Sol. Energy 80 (2006) 1048–1054.
[50] L.C. Chena, Y.J. Tua, Y.S. Wanga, R.S. Kana, C.M. Huang, J. Photochem. Photobiol. A: Chem. 199 (2008) 170–178.
[51] F. Peng, H. Wang, H. Yu, S. Chen, Mater. Res. Bull. 41 (2006) 2123–2129.
[52] L. Jing, Z. Xu, X. Sun, J. Shang, W. Cai, Appl. Surf. Sci. 180 (2001) 308–314.
[53] S. Li, Z. Ma, J. Zhang, Y. Wu, Y. Gong, Catal. Today 139 (2008) 109–112.
[54] P.R. Shukla, S. Wang, M.M. Ang, M.O. Tade, Sep. Pur. Technol. 70 (2010) 338–344.
[55] S.K. Pardeshi, A.B. Patil, J. Mol. Catal. A: Chem. 308 (2009) 32–40.
[56] C. Ye, Y. Bando, G. Shen, D. Golberg, J. Phys. Chem. B 110 (2006) 15146–15151.